Time-Synchronized Laser Induced Fluorescence Techniques for the Study of Quasi-Periodic Xenon Plasma Phenomena

IEPC-2015-349／ISTS-2015-b-349

Presented at Joint Conference of 30th International Symposium on Space Technology and Science, 34th International Electric Propulsion Conference and 6th Nano-satellite Symposium
Hyogo-Kobe, Japan
July 4–10, 2015

Andrea Lucca Fabris,* Christopher V. Young,† and Mark A. Cappelli‡
Stanford Plasma Physics Laboratory, Stanford, CA, 94305, USA

This paper reviews two time-synchronized laser induced fluorescence methods that may be applied to a wide range of periodic and quasi-periodic plasma phenomena. The first approach utilizes a sample-hold technique for restricting collection of the fluorescence signal to small acquisition gates triggered at a particular phase in the oscillation cycle. The averaged signal in each gate is held until the updated value arrives from the next gate one period later. The second is a novel method based on fast switching of the fluorescence signal, again with signal collection occurring in a small sample gate once per oscillation period. Phase sensitive homodyne detection with a lock-in amplifier reduces background noise. We report time-resolved laser induced fluorescence measurements applied to different plasma sources characterized by oscillating plasma structures, either forced or natural. Particularly, we consider a forced AC xenon discharge oscillating at 60 Hz and a Hall thruster naturally oscillating at ∼20 kHz. We present comparisons between the two methods and validate the results against numerical models.

Nomenclature

τ	= sampling gate width for time-synchronized acquisitions
Δt	= time step for time-synchronized acquisitions
e	= elementary charge
n_e	= electron density
n_0	= ground state neutral density
ϵ_e	= electron energy
μ_e	= electron mobility
μ_i	= ion mobility
D_a	= ambipolar diffusion coefficient
$I(t)$	= time-varying discharge current in the AC capillary plasma source
$E(t)$	= time-varying electric field in the AC capillary plasma source
R	= capillary plasma source radius

*Postdoctoral Research Fellow, Mechanical Engineering Department, lfandrea@stanford.edu.
†PhD Candidate, Mechanical Engineering Department, cvyoung@stanford.edu
‡Professor, Mechanical Engineering Department, cap@stanford.edu

I. Introduction

Several plasma sources contain fluctuating structures with varying degrees of periodicity. The development of time-resolved diagnostic techniques is a fundamental step to capture the physics of these phenomena. This paper details the development of laser induced fluorescence (LIF) techniques to measure the time evolution of the ion velocity distribution function in oscillatory plasma sources. In particular, the methods may be applied to forced or natural fluctuations in plasmas exhibiting quasi-steady repeating patterns in time. Forced quasi-periodic phenomena are excited by an external oscillating source (e.g. an oscillating voltage), while natural quasi-periodic phenomena include instabilities and non-linear processes naturally occurring in a plasma under certain conditions.

LIF spectroscopy[1,2] is a reliable and non-intrusive diagnostic that avoids the plasma perturbation that may occur with probe-based techniques. Spectral lineshapes can be accurately measured and plasma properties can be obtained by this analysis. The application of LIF spectroscopy to ion velocimetry involves measuring a Doppler shift in the laser induced fluorescence spectrum of a moving species compared to a stationary reference. Since the ionic transitions are narrow, LIF can nominally measure velocities at 100 m/s resolution. The measurement volume is defined by the intersection of the laser beam and collection optical path, allowing for fine spatial resolution. These advantages make LIF uniquely suited for characterizing the ejected plasma from an accelerator or obtaining the local ion velocity distribution function in a plasma discharge. The most common implementation of LIF is time averaged – the fluorescence photons are collected and integrated over a given time interval – however, developing time-resolved LIF methods has been the subject of recent research effort.

We implement the time-resolved LIF diagnostics described here with an eye towards applications such as measuring the time and spatial evolution of the ion velocity distribution functions in Hall thrusters.[3] These devices exhibit multiple quasi-periodic structures and instabilities[4] that require time-resolved experimental methods to be captured in fine detail. Previous work focused on this task has employed both natural and externally-driven Hall thruster oscillations, depending on the particular method's requirement for coherent oscillations. Vaudolon et al. demonstrated a photon counting technique using a Hall thruster with externally stabilized oscillations.[5] MacDonald et al. resolved the ion velocity distribution function during the natural quasi-periodic 3 kHz discharge current oscillation in a Divergent Cusped Field Thruster[6] and Young et al. extended this approach to track time-resolved ion dynamics in an unforced Hall thruster with 20 kHz natural breathing mode oscillations.[7] Durot et al. also developed a transfer function averaging technique using a hollow cathode discharge, forcing periodic current oscillations at 10 kHz.[8] Finally a heterodyne approach using Fourier decomposition of the LIF signal has been recently proposed by Diallo et al.[9] Various methods have been also developed to address other types of sources, such as pulsed plasmas.[10]

In this paper we present two different LIF methods for obtaining time resolution. The first is the established sample-and-hold scheme,[11] already applied to a Divergent Cusped Field thruster and a Hall thruster operating with a natural breathing mode.[12,13] We will use the sample-and-hold measurements as a benchmark for the validation of a novel technique based on quickly switching the LIF signal on and off. We apply the methods to two plasma sources: a low-frequency (60 Hz) forced oscillating discharge and a Hall thruster operating in a 23 kHz natural breathing mode. Experimental results of the former study will be compared with theoretical predictions from a Collisional-Radiative model in order to provide a physical explanation of the measured time evolution of the probed excited state density.

II. Time-Synchronized Laser Induced Fluorescence Methods

The laser induced fluorescence experimental setup has been extensively described in previous work.[7,14] We summarize here the main hardware components of the system used in these studies. In the text below, all wavelengths are expressed in vacuum. For the 60 Hz oscillatory discharge study, we probe the Xe I (neutral) $6s'[1/2]_1 - 6p'[3/2]_2$ (834.912 nm) transition and we detect the induced fluorescence from the $6s[3/2]^1_0$–$6p'[3/2]_2$ transition at 473.5 nm. For the Hall thruster breathing mode study, the Xe II (ion) $5d[4]_{7/2} - 6p[3]_{5/2}$ (834.953 nm) transition is excited and the resulting fluorescence from the $6s[2]_{3/2}$– $6p[3]_{5/2}$ transition at 542.1 nm is collected for determining the Doppler shift in the absorbed laser radiation.

The exciting laser beam is generated by a New Focus TA-7600 semiconductor tapered amplifier which is seeded by a 20 mW tunable external-cavity diode laser (New Focus, Model TLB-6817-P) through a polarization-maintaining optical fiber. The laser wavelength is determined using a Fabry-Perot interferometer which provides frequency marks (spaced FSR = 1.5 GHz) throughout the scan and a stationary optogalvanic reference signal associated with either the 834.912 nm or the 834.974 nm xenon neutral transitions in a hollow cathode lamp. An additional Burleigh WA-1500 wavemeter is used for a visual wavelength reading while tuning the laser parameters. The fluorescence is collected by a system of lenses and mirrors and detected with a Hamamatsu 1P21 photomultiplier tube (PMT). Before entering the PMT aperture the light is filtered through optical shortpass and bandpass filters in order to reject photons originating from other transitions or from laser beam scattering. A 2 mm mechanical iris reduces the collection volume and defines the ~ 1 mm^3 spatial resolution of the system.

A. Sample-Hold Method

The sample-and-hold method for obtaining time-resolved laser induced fluorescence lineshapes applies to either externally forced or naturally oscillating plasmas and is illustrated in Fig. 1. The oscillation must be quasi-periodic in the sense that the method tolerates a fair amount of frequency drift about the fundamental frequency. The method relies on generating an acquisition gate locked at a given phase of the oscillating period. The LIF signal from the PMT is sampled within this acquisition gate, averaged, and held until the following gate when it is updated (once per period). Through this architecture, only the the LIF contribution originating at the given phase of the oscillation period is processed during a laser wavelength scan, allowing determination of the instantaneous ion velocity distribution function (IVDF). The overall time evolution of the IVDF is then reconstructed from several scans taken at a variety of phases. In order to reduce the acquisition time, the PMT signal can be split into multiple sample-and-hold branches set at different phases in order to simultaneously measure multiple IVDFs during a single wavelength scan.

The acquisition gate is generated by a pulse-delay generator (Stanford Research Systems DG535) triggered by a voltage comparator chip (Model LM339). The latter receives the discharge current signal as an input and produces a positive output for positive values of the discharge current and a null output for negative values. The result is a square wave signal synchronized with a target phase of the discharge current. The sample-and-hold procedure may be implemented through boxcar averaging, a monolithic sample-and-hold chip, or a custom circuit. For the 60 Hz discharge study we use a Texas Instruments LF198 monolithic chip with an RC time constant of 1.75 ms; for the Hall thruster investigation we have designed and built sample-and-hold units satisfying the various requirements of triggering frequency, gate width, and acquisition time for resolving IVDF fluctuations up to 50 kHz.

Homodyne detection, implemented by an SRS 850 locking amplifier, is applied to extract the weak induced fluorescence signal from the bright spontaneous background plasma emission. The laser beam is amplitude-modulated at given frequency f_c through a mechanical chopper before being focused on the plasma, producing a modulation of the LIF signal at the same frequency. The lock-in amplifier extracts the component of the PMT signal at this specific frequency f_c. In the sample and hold method, the chopper frequency f_c is lower than the discharge current fundamental frequency f_0 (typically $f_0/f_c \approx 5-20$) in order to allow multiple sample-and-hold updates within a chopping window.

B. Fast Switching Method

The fast-switching method also resolves the time evolution of the IVDF during quasi-periodic oscillations in plasmas and is summarized in Fig. 1. The oscillation may be externally forced or arise from intrinsic physical processes occurring in the plasma. This method also relies on the generation of an acquisition gate locked at a given phase of the oscillation period. The PMT output is switched on and off according to the acquisition gate: only the signal within the gate is sampled and processed by the lock-in amplifier, while the signal outside the gate is discarded (nulled). The overall time evolution throughout an oscillation cycle is reconstructed from several scans, again parking the acquisition gate at different phases. Homodyne detection is used to extract the induced fluorescence photons from the background plasma emission from the same transition. In this case the chopping frequency is higher than the discharge current fundamental frequency (typically $f_c/f_0 \approx 50 - 100$) in order to provide the lock-in with a clear frequency component at f_c.

C. Method Comparison

For both methods, the time resolution depends on the gate width τ and on the relative delays Δt between consecutive gates. The sample-and-hold approach is more easily implemented at frequencies above 200 Hz.

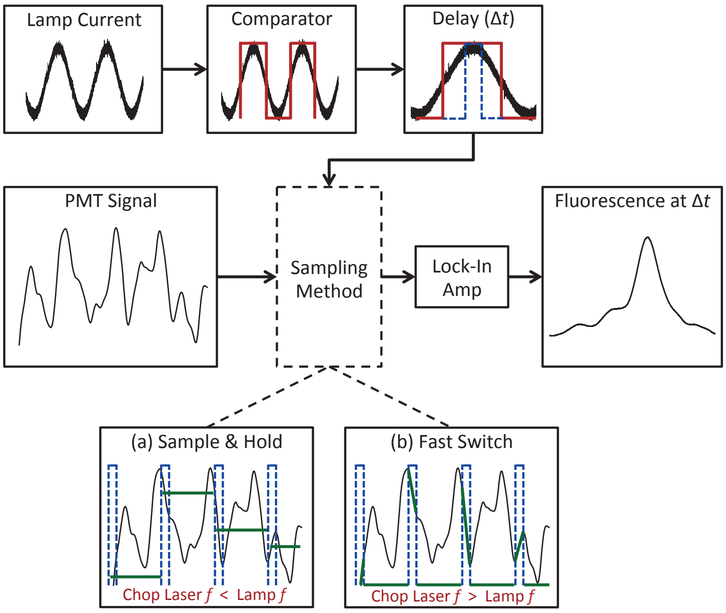

Figure 1. Block diagrams of the (a) sample-and-hold, and (b) fast switching time-synchronization methods for laser induced fluorescence spectroscopy. A comparator triggers the generation of a sampling gate of width τ and delay time Δt from the point at which the discharge current crosses zero with positive slope. The fluorescence signal from the PMT is processed according to each method and fed into a lock-in amplifier, yielding the LIF lineshape at the chosen phase of the current cycle.

The smallest applicable sampling gate is mainly dependent on the hardware used to implement the sample-and-hold architecture. Disadvantages compared with the fast switching method are the more complicated electronics required for processing the LIF signal and the need to chop the laser at frequencies lower than that of the discharge, possibly causing a degradation of the signal-to-noise ratio at low frequencies.

The fast switching method allows for improved noise rejection when studying phenomena at relatively low frequencies (below 200 Hz), since it allows for higher laser chopping frequencies where the spectral noise density is usually lower. However, implementing this method for use with higher frequency phenomena increases in difficulty and hardware cost. For example, if we consider a plasma oscillation at 50 kHz, we would need an acquisition gate of 2 μs or smaller, requiring a chopping frequency of at least a few megahertz. These parameters imply the use of an acousto-optic modulator for chopping the laser and an RF lock-in amplifier for extracting the LIF signal. Moreover, the intensity of the resulting signal is dependent on the on/off duty cycle imposed by the switching. This sets a limitation on the smallest applicable sampling gate and thus restricts the time resolution.

III. Experimental Applications

A. Low Frequency Xenon Discharge with Forced Oscillations

This plasma source is a capillary xenon discharge, 10 cm long and 1.5 mm in diameter, filled to ~7 Torr (estimated from previous lineshape broadening studies).[15] The plasma is driven by hollow electrodes located at the edges of the capillary channel that are powered at 60 Hz. The resulting sinusoidal discharge current has an amplitude of 15 mA and the alternating voltage is about 650 V. We probe the center of the capillary region with 1 mm^3 spatial resolution.

Fig. 2 illustrates the time evolution of the $6s'[1/2]_1 - 6p'[3/2]_2$ (834.912 nm) transition lineshape obtained with the fast switching method. The LIF intensity is representative of the $6s'[1/2]_1$ population density, hereafter labeled as $6s'_1$. The plot on the left shows coarser time resolution measurements with a gate width $\tau = 1$ ms and time steps of 1 ms taken over the full 16.7 ms period. Each lineshape acquired at a given delay time from the trigger constitutes a horizontal slice in the plot. The contour plot is normalized by the overall maximum LIF intensity detected throughout the full current cycle and ranges from 0 (blue) to 1 (red). The

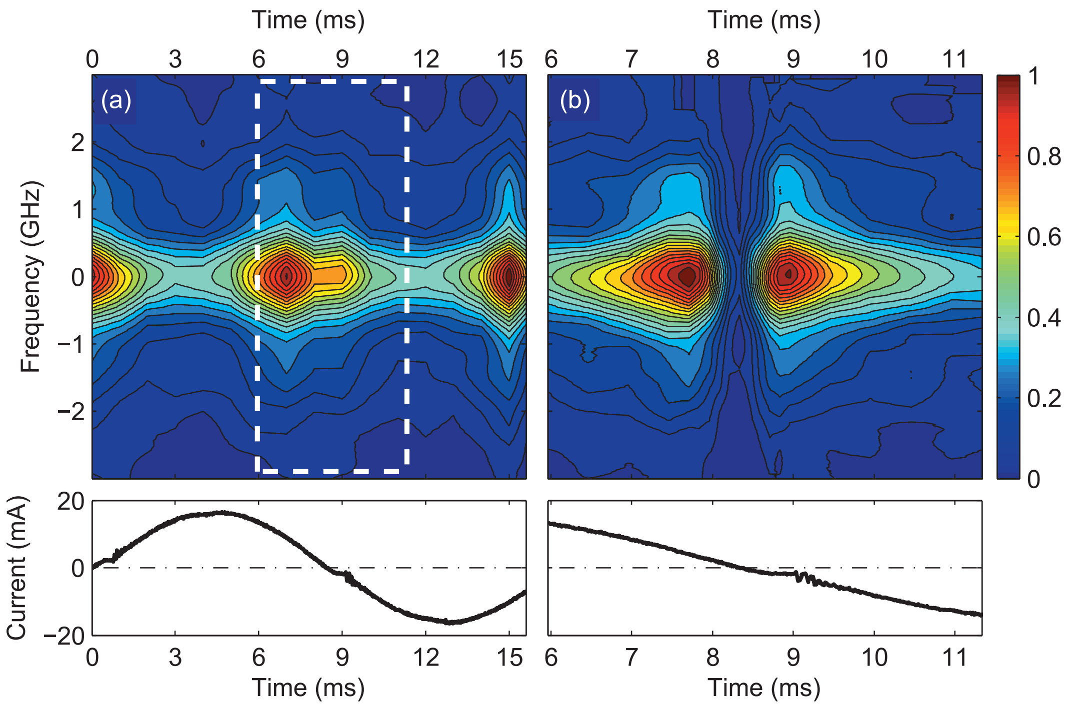

Figure 2. Time evolution of the probed Xe I transition lineshape (834.912 nm) during a discharge current cycle measured with the fast-switching method. (a) LIF traces obtained with a $\tau = 1$ ms gate width and Δt = 1 ms increments throughout the full discharge current cycle. (b) Finer time resolution measurements (0.125 – 0.5 ms increments, 0.5 ms gate width) located near the discharge current zero crossing in which strong temporal gradients are observed.

right panel reports higher time resolution measurements, focusing around the zero-crossing of the discharge current, where strong temporal gradients in the LIF intensity are observed. A gate width of 0.5 ms and a variable time step between 0.125 – 0.5 ms have been used for this purpose. Equivalent contour plots are taken with the sample-hold method (not shown). The laser chopping frequencies used in each case are 17 Hz and 4.6 kHz for the sample-and-hold and fast-switching methods respectively.

The agreement between the two methods is demonstrated in the left panel of Fig. 3, which shows the time variation in the peak fluorescence intensity obtained using each method. The profiles have consistent trends and capture the alternating population and depopulation of the $6s'_1$ excited state density. In particular, the maximum fluorescence intensity (and corresponding $6s'_1$ population density) occurs for a short time at low values of the discharge current, whereas it decreases near the current maximum. Strong quenching of the probed excited state is observed at the current zero crossing. As explained in the next subsection, several physical mechanisms combine to produce this particular time profile: electron-impact excitation and de-excitation, radiative decay, heavy particle collisions and radiation trapping.

1. Comparison with Collisional Radiative Model

A zero-dimensional Collisional-Radiative model is used to reproduce and explain the $6s'_1$ state density profile obtained from the time-resolved LIF measurements. The model is based on a set of xenon atomic energy levels identified by Sommerer.[16] This CR model was previously applied to the positive column of DC plasma discharges and is extended in this work to low-frequency AC discharges. We describe the main characteristics of the model below and will report further details in future publications.

1. The model includes seven neutral excited states and the continuum. Rate equations written for each level balance the incoming and outgoing energy fluxes between allowed transitions with other states. Integrating the rate equations in time provides the time evolution of the excited states' densities during a 60 Hz discharge current cycle.

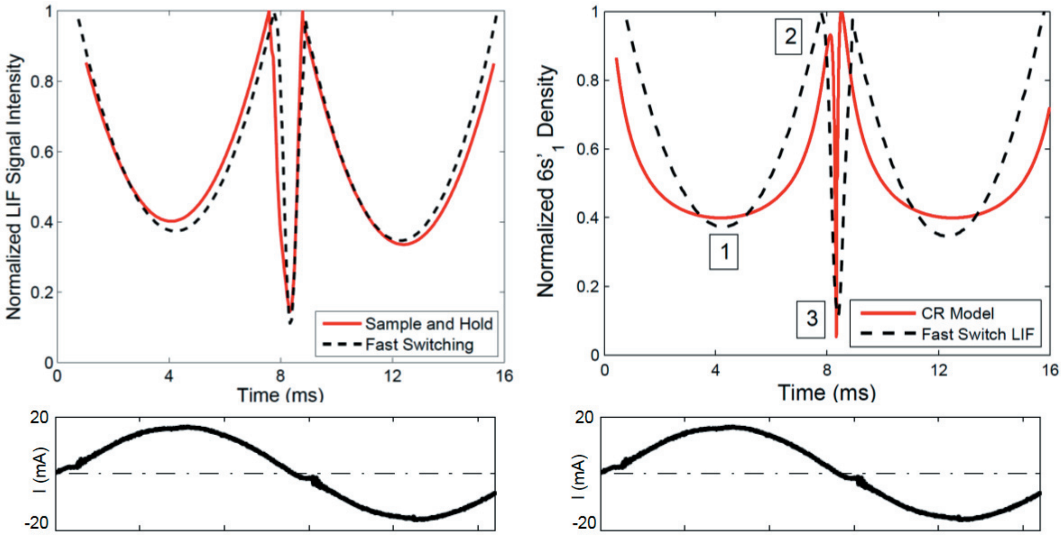

Figure 3. (Left) Time histories of the peak LIF intensity during a 60 Hz current cycle measured through the sample-and-hold and fast-switching methods. The profiles are representative of the time-dependent density of the probed Xe I excited state. (Right) The same profile as predicted by the CR model plotted with the experimental fast-switching trace for comparison. We identify three characteristic regions that are captured by both the model and experiments.

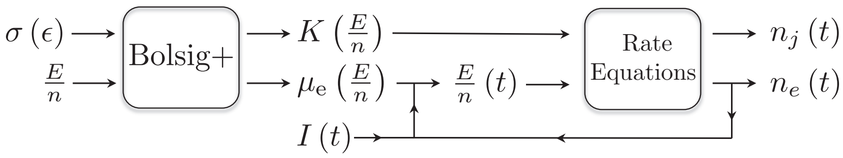

Figure 4. Overall computational loop of the Collisional-Radiative model. The transition rates are calculated by knowing the electron energy distribution function calculated by the external code Bolsig+. The time loop integrates a set of rate equations describing the density evolution of each excited state plus electrons. The equations include time-varying rate coefficients dependent on the local time-varying electric field.

2. The rate coefficients for electron-impact excitation and ionization transitions are calculated using Bolsig+,[17] which solves the zero-dimensional Boltzmann equation using the provided cross-sections. Lookup tables for the rate coefficients and mean electron energy are created for several values of the reduced electric field E/n_0 (where n_0 is the ground state density). Electron-impact de-excitation rates are calculated by applying detailed balance with the corresponding excitation transition.

3. We identify cross-sections describing electron-impact excitation, electron-impact ionization, and heavy particle collisions between excited xenon atoms and radiative decay rates from the literature and account for them in the code.

4. Holstein's theory of radiation trapping is used to estimate effective decay rates of resonant states.[18]

5. Ambipolar diffusion to the cylindrical wall is the main loss mechanism of charged particles. The ambipolar diffusion coefficient is expressed as $D_a \approx 2/3\epsilon_e\mu_i$, where ϵ_e is the electron energy and μ_i the ion mobility.

6. The measured 60 Hz discharge current is input into the code and is used to calculate the time-varying electric field from the electron mobility μ_e: $E(t) = I(t)/(\mu_e e n_e(t)\pi R^2)$, where n_e is the electron density ($n_e = n_i$ for quasi-neutrality), e the elementary charge, and R the discharge radius.

The right panel of Fig. 3 illustrates the time-varying $6s_1'$ excited state density predicted by the numerical model and measured by the time-resolved LIF techniques. Measurements and simulations reproduce the

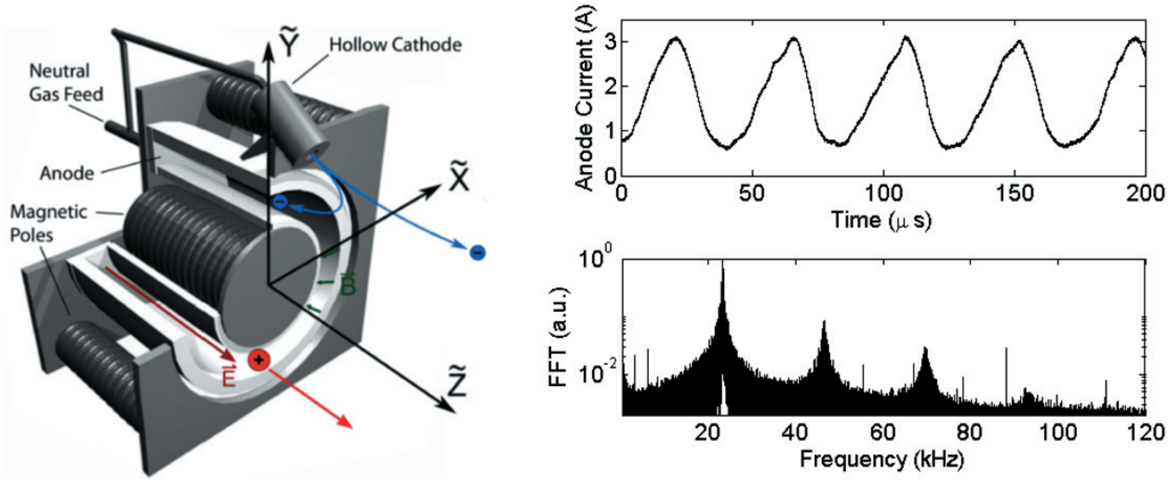

Figure 5. Schematic of the Hall thruster used in this study. The channel centerline is located at $x = 28.5$ mm from the thruster axis. The panel shows the anode current during thruster operation in the breathing mode regime. The FFT highlights the dominant frequency of 23 kHz, along with its harmonics.

same profile characterized by alternating phases of population and de-population of the probed excited state. An analysis of the energy flows between the different excited states and the continuum highlights the physical mechanisms at play. At high values of the discharge current (phase 1), the $6s'_1$ state depopulates due to electron-impact excitation to the upper energy levels. For low values of the discharge current (phase 2), excitation from the lower levels plus radiative decay from the upper states overcome the depopulating processes and increase the $6s'_1$ density up to its maximum observed value. Finally, near the zero crossing of the discharge current (phase 3), the electric field no longer sustains the plasma discharge and all excitation processes halt, resulting in quenching of the excited populations. The sequence then repeats in reverse for the next half period of the oscillation. The model, despite the simplifying assumptions, is able to track the empirical trends and highlights the collisional-radiative mixing between the excited states that act to produce the observed LIF profiles.

B. Naturally Oscillating Hall Thruster

The time-synchronized laser induced fluorescence methods are also demonstrated on a naturally-oscillating Hall thruster. The device has an annular channel with an outer diameter of 72 mm, an inner diameter of 42 mm, and a depth of 23 mm. The thruster is operated at an average power of 408 W (anode voltage 240 V, anode current 1.7 A) with a xenon mass flow rate of 1.97 mg/s. An external IonTech barium oxide cathode (with a 150 μg/s argon propellant feed) is located 2 cm downstream and 7 cm radially outwards from the thruster main axis, pointing at about 45°. The radial magnetic field level at the exit plane on the channel centerline is about 160 G. For these operating conditions the anode current is characterized by regular breathing mode oscillations[12,13] at about 23 kHz, as shown in Fig. 5.

A cryogenic pumping system provides a base pressure of 5×10^{-7} torr and maintains a background pressure of 5×10^{-5} torr (uncorrected for xenon) during thruster operation. We track the time evolution of the ion and neutral velocity distribution functions at several points in the thruster plume, applying the sample-and-hold method. In this work we take a representative point on the channel centerline, 15 mm downstream of the exit plane, to demonstrate the usefulness of the method with drifting natural oscillations. We report extended experimental measurements, for both ions and neutrals, in a separate paper.[19] LIF traces are acquired using $\Delta t = 2.5$ μs increments throughout the discharge current period and a $\tau = 2$ μs measurement gate.

The left panel of Fig. 6 shows the time evolution of the ion velocity distribution function during a single breathing oscillation. Each LIF trace at a given instant is normalized relative to its maximum intensity (a local maximum in time) to properly highlight the dominant ion population throughout the current fluctuation. The right panel shows how the LIF signal intensity changes over time, normalized relative to the

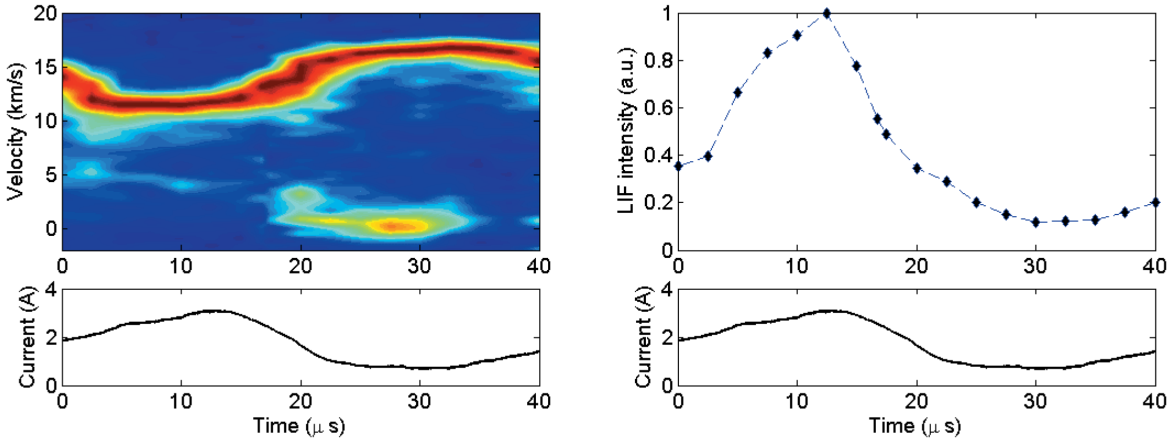

Figure 6. (Left) Time evolution of the ion velocity distribution function during a breathing cycle measured with the sample-hold method at the point $x = 28.5$ mm (channel centerline), and $z = 15$ mm into the plume. The signal intensity varies from 0 (blue) to 1 (red). Each LIF trace at a given instant in time is normalized relative to its maximum intensity to highlight the ion velocity structures appearing at different phases. (Right) LIF signal intensity normalized relative to the global maximum.

global maximum. We observe fluctuations in both velocity and fluorescence intensity, as well as multiple ion populations. The LIF intensity tracks the discharge current profile, peaking at the discharge current maximum, then progressively decreasing until its minimum in the current dip. The ions have a lower velocity at high discharge current values, accelerate during the decreasing ramp of the current, and reach the maximum velocity at low values of the discharge current. In this latter time window a low velocity population is observed in addition to the dominant population at high velocity. Further measurements and analyses are reported separately,[19] along with a physical discussion of the observed processes.

IV. Summary and Future Work

This paper describes and compares two different time-resolved laser induced fluorescence techniques for studying quasi-periodic plasmas based on a sample-and-hold and fast-switching approach. First, the methods are applied to a low-frequency (60 Hz) forced-oscillating xenon discharge, giving consistent results when reconstructing the time-evolution of the neutral xenon $6s'[1/2]_1 - 6p'[3/2]_2$ (834.912 nm) transition lineshape. Experimental measurements are compared with collisional-radiative simulations of the probed plasma, yielding a similar picture of the time history of the probed excited state density. The numerical analysis highlights the physical mechanisms of collisional and radiative mixing, radiation trapping and electron impact ionization that combine to determine the overall time-varying behavior of the excited states.

We also report time-resolved ion velocity measurements in a Hall thruster operating with a 23 kHz breathing mode obtained using the sample-hold approach. Strong ion velocity and fluorescence intensity fluctuations are observed throughout the breathing mode cycle, along with multiple ion populations that arise during certain phases. Future work will compare the various time-resolved LIF methods reported in the literature and further investigate the dynamics of Hall thruster discharges by applying a combination of LIF measurements and numerical models.

Acknowledgments

This work is sponsored by the Lawrence Livermore National Laboratory and the U.S. Air Force Office of Scientific Research with Dr. M. Birkan as program manager. C.Y. acknowledges support from the DOE NSSA Stewardship Science Graduate Fellowship under contract DE-FC52-08NA28752 and the Stanford Graduate Fellowship.

References

[1]Skiff, F. and Bollinger, J., "Mini-conference on laser-induced fluorescence in plasmas," *Physics of Plasmas*, Vol. 11, No. 5, 2004, pp. 2972–2975.

[2]Hargus Jr, W. and Cappelli, M., "Laser-induced fluorescence measurements of velocity within a Hall discharge," *Applied Physics B*, Vol. 72, No. 8, 2001, pp. 961–969.

[3]Cappelli, M., "The Hall effect and rocket flight," *Physics Today*, Vol. 62, No. 4, 2009, pp. 76–77.

[4]Choueiri, E., "Plasma oscillations in Hall thrusters," *Physics of Plasmas*, Vol. 8, No. 4, 2001, pp. 1411–1426.

[5]Vaudolon, J., Balika, L., and Mazouffre, S., "Photon counting technique applied to time-resolved laser-induced fluorescence measurements on a stabilized discharge," *Review of Scientific Instruments*, Vol. 84, No. 7, 2013, pp. 073512.

[6]MacDonald, N., Cappelli, M., and Hargus Jr, W., "Time-synchronized continuous wave laser-induced fluorescence axial velocity measurements in a diverging cusped field thruster," *Journal of Physics D: Applied Physics*, Vol. 47, No. 11, 2014, pp. 115204.

[7]Young, C. V., Lucca Fabris, A., and Cappelli, M. A., "Ion dynamics in an $E \times B$ Hall plasma accelerator," *Applied Physics Letters*, Vol. 106, No. 4, February 2015, pp. 044102.

[8]Durot, C., Gallimore, A., and Smith, T., "Validation and evaluation of a novel time-resolved laser-induced fluorescence technique," *Review of Scientific Instruments*, Vol. 85, No. 1, 2014, pp. 013508.

[9]Diallo, A., Keller, S., Shi, Y., Raitses, Y., and Mazouffre, S., "Time-resolved ion velocity distribution in a cylindrical Hall thruster: Heterodyne-based experiment and modeling," *Review of Scientific Instruments*, Vol. 86, No. 3, 2015, pp. 033506.

[10]Biloiu, I. A., Sun, X., and Scime, E. E., "High time resolution laser induced fluorescence in pulsed argon plasma," *Review of Scientific Instruments*, Vol. 77, No. 10, 2006, pp. 10F301.

[11]MacDonald, N., Cappelli, M., and Hargus Jr, W., "Time-synchronized continuous wave laser-induced fluorescence on an oscillatory xenon discharge," *Review of Scientific Instruments*, Vol. 83, No. 11, 2012, pp. 113506.

[12]Boeuf, J.-P. and Garrigues, L., "Low frequency oscillations in a stationary plasma thruster," *Journal of Applied Physics*, Vol. 84, No. 7, 1998, pp. 3541.

[13]Barral, S. and Ahedo, E., "Low-frequency model of breathing oscillations in Hall discharges," *Physical Review E*, Vol. 79, No. 4, 2009, pp. 046401.

[14]Fabris, A. L., Young, C. V., Manente, M., Pavarin, D., and Cappelli, M. A., "Ion Velocimetry Measurements and Particle-In-Cell Simulation of a Cylindrical Cusped Plasma Accelerator," *IEEE Transactions on Plasma Science*, Vol. 43, No. 1, 2015, pp. 54–63.

[15]MacDonald, N. A., *Laser induced fluorescence characterization of cusped field plasma thrusters*, Ph.D. thesis, Stanford University, 2012.

[16]Sommerer, T. J., "Model of a weakly ionized, low-pressure xenon dc positive column discharge plasma," *Journal of Physics D: Applied Physics*, Vol. 29, No. 3, 1996, pp. 769.

[17]Hagelaar, G. and Pitchford, L., "Solving the Boltzmann equation to obtain electron transport coefficients and rate coefficients for fluid models," *Plasma Sources Science and Technology*, Vol. 14, No. 4, 2005, pp. 722.

[18]Holstein, T., "Imprisonment of resonance radiation in gases," *Phys. Rev.*, Vol. 72, No. 12, Dec 1947, pp. 1212–1233.

[19]Young, C. V., Lucca Fabris, A., and Cappelli, M. A., "Time-Synchronized Laser Induced Fluorescence Measurement of Xenon Ion and Neutral Dynamics in a 350 W Hall Thruster," *Proceedings of the 34th Internationl Electric Propulsion Conference*, 2015, pp. IEPC–2015–437p.